Syntheses, Structures, Bonding, and Redox Behavior of 1,4-Bis(ferrocenyl)butadiyne Coordinated Osmium Clusters

Richard D. Adams,*,† Bo Qu,† Mark D. Smith,† and Thomas A. Albright‡

Department of Chemistry and Biochemistry and The USC Nanocenter, University of South Carolina, Columbia, South Carolina 29208, and Department of Chemistry, University of Houston, Houston, Texas 77204

Received February 14, 2002

Downloaded by CARLI CONSORTIUM on June 29, 2009
Published on May 25, 2002 on http://pubs.acs.org | doi: 10.1021/om0201213

The reaction of $Os_3(CO)_{11}(NCMe)$ (**1**) with 1,4-bis(ferrocenyl)butadiyne (**3**) yielded two products: $Os_3(CO)_{10}(\mu_3\text{-}\eta^2\text{-}FcC_4Fc)$ (**4**) and $Os_3(CO)_{11}(\mu_3\text{-}\eta^4\text{-}FcC_4Fc)$ (**5**). Compound **4** was obtained in better yield (94%) from the reaction of $Os_3(CO)_{10}(NCMe)_2$ (**2**) with **3** at 67 °C. Compound **4** contains a bis(ferrocenyl)butadiyne ligand coordinated to a triangular triosmium cluster via one of its alkyne groups in a triply bridging fashion. Compound **5** contains an open triosmium cluster with the two C−C triple bonds coordinated in a parallel fashion to the three metal atoms. Compound **2** reacts with **3** at 97 °C to yield the compound $Os_2(CO)_6(\mu\text{-}\eta^4\text{-}FcC_2C{\equiv}CFc)_2$ (**6**) as a result of cluster fragmentation. Compound **6** exhibits a ferrole-type structure formed by the coupling two molecules of diyne **3**. At 97 °C **4** is transformed into the new compound $Os_3(CO)_9(\mu_3\text{-}\eta^2\text{-}C{\equiv}CFc)(\mu\text{-}\eta^2\text{-}C{\equiv}CFc)$ (**7**), which contains two bridging ferrocenylacetylide ligands formed by cleaving the C−C bond between the two alkyne groups. All four products were characterized by IR, ^{1}H NMR, and single-crystal X-ray diffraction analyses. The two ferrocenyl units in **4**, **6**, and **7** are inequivalent. The redox potentials of the ferrocenyl groups in **4** are very closely spaced, $\Delta E_p = 0.057$ V, suggesting that there is little electrocommunication between them. The redox potentials of the ferrocenyl groups in **6** are widely spaced, probably due to their intrinsic inequivalence. The two ferrocenyl units in **5** are equivalent but show two resolved one-electron redox processes, $\Delta E_p = 0.184$ V, which indicates that there is significant electrocommunication between them. This is attributed to greater interactions in the π-orbital network in the ligand **3** induced by coordination to the metal atoms. A molecular orbital model based on a butatrienediyl group is proposed to explain the coordination and π-bonding in the 1,4-bis(ferrocenyl)butadiyne ligand in **5**.

Introduction

Molecules containing long chains of unsaturated atoms capable of transmitting electrons have been proposed for use as molecular wires for the construction of nanoscale electronic devices.[1,2] Recently, there has been much interest in the coordination chemistry of conjugated di- and polyynes.[3] Conjugated polyynes appear to be especially effective in facilitating electronic exchange.[1] Electronic communication through such potential molecular wires is often evaluated by examining the redox response of electroactive groups placed at their terminii.[1]

We have now prepared and characterized several new osmium complexes by the reactions of the triosmium carbonyl cluster complexes $Os_3(CO)_{11}(NCMe)$ (**1**) and $Os_3(CO)_{10}(NCMe)_2$ (**2**) with 1,4-bis(ferrocenyl)butadiyne (**3**). Changes in the redox potentials of the ferrocenyl groups indicate that the electronic communication between them is strongly effected by the mode of coordination of the metal atoms. The electrocommunication is decreased when a single C−C triple bond is coordinated to the triangle of metal atoms, as observed in the compound $Os_3(CO)_{10}(\mu_3\text{-}\eta^2\text{-}FcCCCCFc)$ (**4**; Fc = $C_5H_4FeC_5H_5$), but it is increased when the triosmium group is coordinated parallel to the polyyne chain, as

* To whom correspondence should be addressed. E-mail: Adams@mail.chem.sc.edu.
† University of South Carolina.
‡ University of Houston.

(1) (a) Paul, F.; Lapinte, C. *Coord. Chem. Rev.* **1998**, *178−180*, 431. (b) Ward, M. D. *Chem. Soc. Rev.* **1995**, 121. (c) Barlow, S.; O'Hare, D. *Chem. Rev.* **1997**, *97*, 637. (d) Grosshenny, V.; Harriman, A.; Hissler, M.; Ziessel, R. *Platinum Met. Rev.* **1996**, *40*, 26. (e) Grosshenny, V.; Harriman, A.; Hissler, M.; Ziessel, R. *Platinum Met. Rev.* **1996**, *40*, 72. (f) Kheradmandan, S.; Heinze, K.; Schmalle, H. W.; Berke, H. *Angew. Chem., Int. Ed.* **1999**, *38*, 2270. (g) Dembinski, R.; Bartik, T.; Bartik, B.; Jaeger, M.; Gladysz, J. A. *J. Am. Chem. Soc.* **2000**, *122*, 810. (h) Tarraga, A.; Molina, P.; Curiel, D.; Desamparados Velasco, M. *Organometallics* **2001**, *20*, 2145. (i) Engtrakul, C.; Sita, L. R. *Nano Lett.* **2001**, *1*, 541.

(2) (a) *Molecular Electronics: Science and Technology*; Aviram, A., Ed.; Conference Proceedings No. 262; American Institute of Physics: New York, 1992. (b) *Molecular and Biomolecular Electronics*; Birge, R. R., Ed.; Advances in Chemistry Series 240; American Chemical Society: Washington, DC, 1991. (c) *Nanostructures and Mesoscopic Systems*; Kirk, W. P., Reed, M. A., Eds.; Academic: New York, 1992. (d) Astruc, D. *Electron Transfer and Radical Processes in Transition-Metal Chemistry*; VCH: New York, 1995; Chapter 4. (e) Collier, C. P.; Wong, E. W.; Belohradsky, M.; Raymo, F. M.; Stoddart, J. F.; Kuekes, P. J.; Williams, R. S.; Heath, J. R. *Science* **1999**, *285*, 391. (f) Feldheim, D.; Keating, C. D. *Chem. Soc. Rev.* **1998**, *27*, 1. (g) Andres, R. P.; Bielefeld, J. D.; Henderson, J. I.; Janes, D. B.; Kolagunta, V. R.; Kubiak, C. P.; Mahoney, W. J.; Osifchin, R. G. *Science* **1996**, *273*, 1690.

(3) Low, P. J.; Bruce, M. I. *Adv. Organomet. Chem.* **2001**, *48*, 71.

10.1021/om0201213 CCC: $22.00 © 2002 American Chemical Society
Publication on Web 05/25/2002

observed in the compound $Os_3(CO)_{11}(\mu_3\text{-}\eta^4\text{-FcCCCCFc})$ (**5**). A bonding model based on the butatrienediyl ligand has been proposed to explain this effect for the latter compound. A preliminary report of this work has been published.[4]

Experimental Section

General Data. Although the reagents and products are air-stable, all the reactions were performed under an atmosphere of nitrogen, unless otherwise indicated. Reagent grade solvents were freshly distilled prior to use. $Os_3(CO)_{11}(NCMe)$[5] (**1**), $Os_3(CO)_{10}(NCMe)_2$[5] (**2**), and 1,4-bis(ferrocenyl)butadiyne[6] (**3**) were prepared according to literature procedures. Separation of the products was achieved by TLC in air on Analtech 0.25 mm silica gel 60 Å F_{254} glass plates. Infrared spectra were recorded on a Nicolet 5 DXBO FT-IR spectrophotometer. ^{1}H NMR spectra were run on a Varian Inova AM-300 spectrometer operating at 300 MHz. Elemental analyses were performed by Desert Analytics, Tucson, AZ, and by Oneida Research Services, Whitesboro, NY. Extended Hückel calculations[7] were performed by using the modified Wolfsberg−Helmholtz formula.[8] The H_{ii} and orbital exponents were taken from the literature.[7b,9]

Reaction of $Os_3(CO)_{11}(NCMe)$ (1) with 1,4-Bis(ferrocenyl)butadiyne (3). A 20.0 mg amount of **1** (0.0217 mmol) and a 9.5 mg amount of **3** (0.0227 mmol) were dissolved in 30 mL of hexane in a 50-mL three-necked round-bottom flask, and the solution was heated to reflux for 20 min. The solvent was then removed in vacuo, and the residue was dissolved in a minimal amount of CH_2Cl_2 and the solution separated by TLC on silica gel by using a hexane/CH_2Cl_2 (3/1) solvent mixture. The principal products (in order of elution) were as follows: 5.1 mg of orange $Os_3(CO)_{10}(\mu_3\text{-}\eta^2\text{-FcC}_4\text{Fc})$ (**4**; 18% yield) and 8.8 mg of red $Os_3(CO)_{11}(\mu_3\text{-}\eta^4\text{-FcC}_4\text{Fc})$ (**5**; 31% yield), Fc = $(C_5H_5)Fe(C_5H_4)$. Data for **4** are as follows. IR (ν_{CO}, cm^{-1}; in hexane): 2097 (s), 2065 (vs), 2055 (vs), 2026 (s), 2014 (sh), 2007 (s), 1982 (w) 1840 (w). ^{1}H NMR (δ; in $CDCl_3$): 4.24 (s, 5H, Cp), 4.28 (s, 5H, Cp), 4.23−4.27 (m, 4H, C_5H_4), 4.30 (m, 2H, C_5H_4), 4.42 (m, 2H, C_5H_4). Anal. Calcd (found): C, 32.19 (31.88); H, 1.42 (1.04). Data for **5** are as follows. IR (ν_{CO}, cm^{-1}; in hexane): 2123 (m), 2095 (s), 2044 (vs), 2040 (sh), 2000 (s), 1969 (w), 1957 (m). ^{1}H NMR (δ; in $CDCl_3$): 4.17 (s, 10H, 2Cp), 4.44 (m, 4H, C_5H_4), 4.61 (m, 4H, C_5H_4). Anal. Calcd (found): C, 32.42 (32.01); H, 1.39 (1.15).

Reaction of 2 with 3 at 68 °C. A 25.0 mg amount of **2** (0.0268 mmol) and a 11.6 mg amount of **3** (0.0277 mmol) were dissolved in 40 mL of hexane in a 100 mL three-necked round-bottom flask. The solution was heated to reflux for 20 min. The solvent was removed in vacuo, the residue was dissolved in a minimal amount of CH_2Cl_2, and the solution was separated by TLC using a hexane/CH_2Cl_2 (4/1) solvent mixture. This gave 32 mg of **4**, in 94% yield.

Reaction of 2 with 3 at 97 °C. A 20.0 mg amount of **2** (0.0214 mmol) and a 26.0 mg amount of **3** (0.0622 mmol) were dissolved in 40 mL of heptane in a 100 mL three-necked round-bottom flask. The solution was heated to reflux for 6 h. The solvent was then removed in vacuo, the residue was dissolved in a minimal amount of CH_2Cl_2, and the solution was separated by TLC using a hexane/CH_2Cl_2 (4/1) solvent mixture. This yielded 3.0 mg of unreacted **3** and 2.7 mg of orange $Os_2(CO)_6(\mu_4\text{-}\eta^4\text{-FcC}_2\text{C}{\equiv}\text{CFc})_2$ (**6**; 9% yield), along with traces of uncharacterizable orange compounds. Analytical and spectral data for **6** are as follows. IR (ν_{CO}, cm^{-1}; in hexane): 2077 (s), 2049 (vs), 2010 (s), 1997 (s), 1982 (m), 1971 (s). ^{1}H NMR (δ; in C_6D_6): 3.99−4.01 (m, 6H, 2 C_5H_4), 4.05 (m, 2H, C_5H_4), 4.19 (s, 10H, 2Cp), 4.22 (s, 10H, 2Cp), 4.28 (m, 2H, C_5H_4), 4.52−5.53 (m, 2H, C_5H_4), 4.55−4.56 (m, 2H, C_5H_4), 4.70 (m, 2H, C_5H_4). Anal. Calcd (found): C, 46.80 (46.85); H, 2.83 (2.60).

Thermolysis of 4. An 18.0 mg amount of **4** was dissolved in 25 mL of heptane in a three-necked round-bottom flask. The mixture was heated to reflux for 3.5 h. After the mixture was cooled, the solvent was removed in vacuo, the residue was dissolved in a minimal amount of CH_2Cl_2, and the solution was separated by TLC by using a hexane/CH_2Cl_2 (4/1) solvent mixture. This gave 16.0 mg of red $Os_3(CO)_9(\mu_3\text{-}\eta^2\text{-C}{\equiv}\text{CFc})(\mu\text{-}\eta^2\text{-C}{\equiv}\text{CFc})$ (**7**; 91% yield). Analytical and spectral data for **7** are as follows. IR (ν_{CO}, cm^{-1}; in CH_2Cl_2): 2088 (w), 2066 (s), 2041 (s), 2006 (s), 1964 (m). ^{1}H NMR (δ; in CD_2Cl_2): 4.16 (s, 5H, Cp), 4.19 (s, 5H, Cp), 4.32−4.33 (m, 2H, C_5H_4), 4.36−4.40 (m, 4H, C_5H_4), 4.50−4.51 (m, 2H, C_5H_4). Anal. Calcd (found): C, 31.94 (32.47); H, 1.46 (1.10).

Crystallographic Analyses. Red crystals of **4** and dark red crystals of **5** were grown by slow evaporation of the solvent from solutions of the compounds in hexane/CH_2Cl_2 (5:1) solvent mixtures at 25 °C. Orange-red crystals of **6** were grown by slow evaporation of the solvent from a solution in hexane/CH_2Cl_2 (4:1) at −20 °C. Red crystals of **7** were grown by slow evaporation of the solvent from a solution in benzene/octane (3:1) at 25 °C.

The data crystals of **4**, **5**, and **7** were mounted in thin-walled glass capillaries. Diffraction measurements on **4** and **7** were made on a Rigaku AFC6S fully automated four-circle diffractometer using graphite-monochromated Mo Kα radiation at 20 °C. Unit cells were determined and refined from 15 randomly selected reflections obtained by using the AFC6 automatic search, center, index, and least-squares routines. Crystal data, data collection parameters, and results of the analyses are listed in Table 1. The data were processed on a Silicon-Graphics *INDIGO*^{2} Workstation by using the TEXSAN structure solving program library obtained from the Molecular Structure Corp., The Woodlands, TX. Neutral-atom scattering factors were calculated by the standard procedures.[10a] Anomalous dispersion corrections were applied to all non-hydrogen atoms.[10b] Lorentz/polarization (Lp) corrections were applied to the data. Full-matrix least-squares refinements minimized the function $\sum_{hkl} w(|F_o| - |F_c|)^2$, where $w = 1/\sigma(F)^2$, $\sigma(F) = \sigma(F_o^2)/2F_o$, and $\sigma(F_o^2) = [\sigma(I_{raw})^2 + (0.06I_{net})^2]^{1/2}/Lp$.

The crystal of **6** was glued onto the end of a thin glass fiber. X-ray intensity data for compounds **5** and **6** were measured at 293 K on a Bruker SMART APEX CCD-based diffractometer using Mo Kα radiation (λ = 0.717 03 Å). The unit cells were determined on the basis of reflections collected from a set of three frames measured in orthogonal wedges of reciprocal space. Crystal data, data collection parameters, and results of the analyses are listed in Table 1. The raw intensity data frames were integrated with the SAINT+ program using a narrow-frame integration algorithm.[11] Corrections for Lorentz and polarization effects were also applied by SAINT. An empirical absorption correction based on the multiple measurement of equivalent reflections was applied by using the program SADABS.

Compounds **4**, **5**, and **7** crystallized in the monoclinic crystal system. The space group $P2_1/a$ was established for **4** on the basis of the systematic absences observed during the collection

Downloaded by CARLI CONSORTIUM on June 29, 2009
Published on May 25, 2002 on http://pubs.acs.org | doi: 10.1021/om0201213

(4) Adams, R. D.; Qu, B. *Organometallics* **2000**, *19*, 2411.
(5) Drake, S. R.; Khattar, R. *Organomet. Synth.* **1988**, *4*, 234.
(6) Rodriguez, J.-G.; Oñate, A.; Martin-Villamil, R. M.; Fonseca. I. *J. Organomet. Chem.* **1996**, *513*, 71.
(7) (a) Hoffmann, R. *J. Chem. Phys.* **1963**, *39*, 1397. (b) Hoffmann, R.; Lipscomb, W. M. *J. Chem. Phys.* **1962**, *36*, 3179; **1962**, *37*, 2872. (c) Our calculations were carried out with the CAESAR program package (Ren, J.; Liang, W.; Whangbo, M.-H. Crystal and Electronic Structure Analyzer, 1998; see http://www.PrimeC.com).
(8) (a) Wolfsberg, M.; Helmholz, L. *J. Chem. Phys.* **1952**, *20*, 837. (b) Ammeter, J. H.; Burgi, H.-B.; Thibeault, J. C.; Hoffmann, R. *J. Am. Chem. Soc.* **1978**, *100*, 3686.
(9) Chen, M. M. L.; Hoffmann, R. *J. Am. Chem. Soc.* **1976**, *98*, 1647.
(10) (a) *International Tables for X-ray Crystallography*; Kynoch Press: Birmingham, England, 1975; Vol. IV, Table 2.2B, pp 99−101. (b) Table 2.3.1, pp 149−150.
(11) SAINT+, Version 6.02a; Bruker Analytical X-ray System, Inc., Madison, WI, 1998.

Table 1. Crystallographic Data for Compounds 4−7

	4	5	6	7
empirical formula	$Os_3Fe_2O_{10}C_{34}H_{18}$	$Os_3Fe_2O_{11}C_{35}H_{18}\cdot 0.5CH_2Cl_2$	$Os_2Fe_4O_6C_{54}H_{36}$	$Os_3Fe_2O_9C_{33}H_{18}$
fw	1268.80	1339.26	1384.63	1240.79
cryst syst	monoclinic	monoclinic	triclinic	monoclinic
lattice params				
a (Å)	15.074(3)	22.4780(11)	12.633(1)	38.952(11)
b (Å)	10.254(3)	7.3654(4)	14.434(2)	9.242(2)
c (Å)	23.055(5)	43.513(2)	15.843(2)	18.576(3)
α (deg)	90.0	90.0	64.948(2)	90.0
β (deg)	103.75(2)	95.782(1)	79.115(2)	102.60(2)
γ (deg)	90.0	90.0	74.266 (2)	90.0
V (Å^3)	3461.70 (7)	7167.3(6)	2509.9 (5)	6526.3 (23)
space group	$P2_1/a$ (No. 14)	$C2/c$ (No. 15)	$P\bar{1}$ (No. 2)	$C2/c$ (No. 15)
Z	4	8	2	8
ρ_{calcd} (g/cm^3)	2.43	2.482	1.832	2.53
μ(Mo Kα) (mm^{-1})	11.84	11.53	6.215	12.55
$2\theta_{max}$ (deg)	44.1	43.1	50.22	44
no. of obsd rflns ($I > 3\sigma(I)$)	3233	7794 ($I > 2\sigma(I)$)	5846 ($I > 2\sigma(I)$)	3057
no. of variables	438	455	587	409
goodness of fit	1.11	1.247	1.016	1.50
max shift in cycle	0.01	0.001	0.001	0.01
residuals: R; R_w[a]	0.0405; 0.0522	0.0445; 0.1096	0.049; 0.118	0.051; 0.070
abs cor	DIFABS	SADABS	SADABS	DIFABS
transmissn coeff: max/min	1.00/0.14	1.000/0.354	0.901/0.735	1.00/0.39
largest peak in final diff map (e/Å^3)	1.47	1.232	1.596	1.92

[a] $R = \sum_{hkl}(||F_o| - |F_c||)/\sum_{hkl}|F_o|$; $R_w = [\sum_{hkl}w(|F_o| - |F_c|)^2/\sum_{hkl}wF_o^2]^{1/2}$, $w = 1/\sigma^2(F_o)$; GOF $= [\sum_{hkl}(w(|F_o| - |F_c|))^2/(n_{data} - n_{variables})]^{1/2}$.

Downloaded by CARLI CONSORTIUM on June 29, 2009
Published on May 25, 2002 on http://pubs.acs.org | doi: 10.1021/om0201213

of the data. For **5** and **7** the systematic absences were consistent with either of the space groups *Cc* and *C*2/*c*. The latter was selected initially and confirmed by the successful solution and refinement of the structures in both cases. Each of these structures were solved by a combination of direct methods (SIR92) and difference Fourier syntheses. For all three analyses all non-hydrogen atoms were refined with anisotropic thermal parameters. The positions of the hydrogen atoms were calculated and included in the structure factor calculations without refinement.

Compound **6** crystallized in the triclinic crystal system. The space group $P\bar{1}$ was assumed and confirmed by the successful solution and refinement of the structure. The structure was solved by a combination of direct methods and difference Fourier syntheses and refined by full-matrix least squares on F^2, using the SHELXTL software package.[12] All non-hydrogen atoms were refined with anisotropic displacement parameters. Hydrogen atoms were placed in idealized positions and were included in the structure factor calculations without refinement.

Electrochemical Measurements. Cyclic and differential pulse voltammetric measurements (DPV) were performed by using a three-electrode system consisting of a glassy-carbon working electrode, a platinum counter electrode, and a Ag/AgCl reference electrode on a CV-50W voltammetric analyzer purchased from Bioanalytical Systems, West Lafayette, IN. Samples were prepared in 1.0 mM solutions by using a CH_2Cl_2/MeCN (1/1) solvent containing 0.1 M tetrabutylammonium hexafluorophosphate. The DPV potential values are reported as the peak positions E_p. The relationship between the peak potentials in DPV and $E_{1/2}$ values has been described by Richardson et al.[13] Under these conditions E_p for ferrocene is 320 mV (using a pulse amplitude of 10 mV). The DP voltammogram of compound **4** shows two poorly resolved one-electron oxidations for the ferrocenyl groups at $E = 0.483$ and 0.540 V vs Ag/AgCl; $\Delta E_p = 0.057$ V. The DP voltammogram of compound **5** exhibits two very spaced one-electron oxidations for the ferrocenyl groups at $E = 0.300$ and 0.484 V vs Ag/AgCl; $\Delta E_p = 0.184$ V. The DP voltammogram of compound **6** shows two oxidation peaks at different intensities at $E = 0.364$ V (shoulder) and 0.512 V (broad) vs Ag/AgCl; $\Delta E_p = 0.148$ V. The cyclic voltammmogram shows that the former peak is not fully reversible. The DP voltammogram of compound **7** shows two resolved one-electron oxidations for the ferrocenyl groups at $E = 0.43$ and 0.65 V vs Ag/AgCl,; $\Delta E_p = 0.22$ V. The cyclic voltammograms of compounds **4**, **5**, and **7** showed that these redox processes were completely reversible (see the Supporting Information).

Results

The reaction of $Os_3(CO)_{11}$(NCMe) (**1**) with 1,4-bis(ferrocenyl)butadiyne (**3**) yielded two new products: $Os_3(CO)_{10}(\mu_3\text{-}FcC_4Fc)$ (**4**) in 18% yield and $Os_3(CO)_{11}(\mu_3\text{-}FcC_4Fc)$ (**5**) in 31% yield, as shown in Scheme 1. Compound **4** was obtained in a much better yield (94%) from the reaction of **2** with **3** at 68 °C. Compounds **4** and **5** were characterized by IR, ^{1}H NMR, single-crystal X-ray diffraction analyses, and differential pulse voltammetry (DPV). ORTEP diagrams of molecular structures of **4** and **5** are shown in Figures 1 and 2, respectively. Selected interatomic distances and angles of compounds **4** and **5** are listed in Table 2. In **4** a triangular $Os_3(CO)_{10}$ cluster is attached to one of the two C−C triple bonds of the ligand **3**. The second alkyne group is uncoordinated. This coordinated alkyne group exhibits the di-($\sigma + \pi$) coordination mode that is commonly observed for alkynes coordinated to 48e trimetal clusters.[14] As expected, the coordinated triple bond in **3**, C(1)−C(2), is significantly longer than the uncoordinated triple bond C(3)−C(4): C(1)−C(2) = 1.40(2) Å and C(3)−C(4) = 1.19(2) Å. Compound **5** contains an open linear $Os_3(CO)_{11}$ cluster attached both of the C−C triple bonds of the ligand **3** in parallel coordination. Both C−C multiple bonds in the ligand are lengthened upon coordination: (C(1)−C(2) = 1.328(11) Å, C(3)−C(4) = 1.319(12) Å), while the C(2)−C(3) single bond is shortened to 1.324(11) Å. The molecule **5** has approximate mirror symmetry (not crystallographic), which was confirmed by the observation of a single resonance

(12) Sheldrick, G. M. SHELXTL, Version 5.1; Bruker Analytical X-ray Systems, Inc., Madison, WI, 1997.

(13) Richardson, D. E.; Taube, H. *Inorg. Chem.* **1981**, *20*, 1278.

(14) (a) Deabate, S.; Giordano, R.; Sappa, E. *J. Cluster Sci.* **1997**, *8*, 407. (b) Deeming, A. J. *Adv. Organomet. Chem.* **1986**, *26*, 1. (c) Raithby, P. R.; Rosales, M. *Adv. Inorg. Chem. Radiochem.* **1985**, *29*, 169.

Downloaded by CARLI CONSORTIUM on June 29, 2009
Published on May 25, 2002 on http://pubs.acs.org | doi: 10.1021/om0201213

Scheme 1

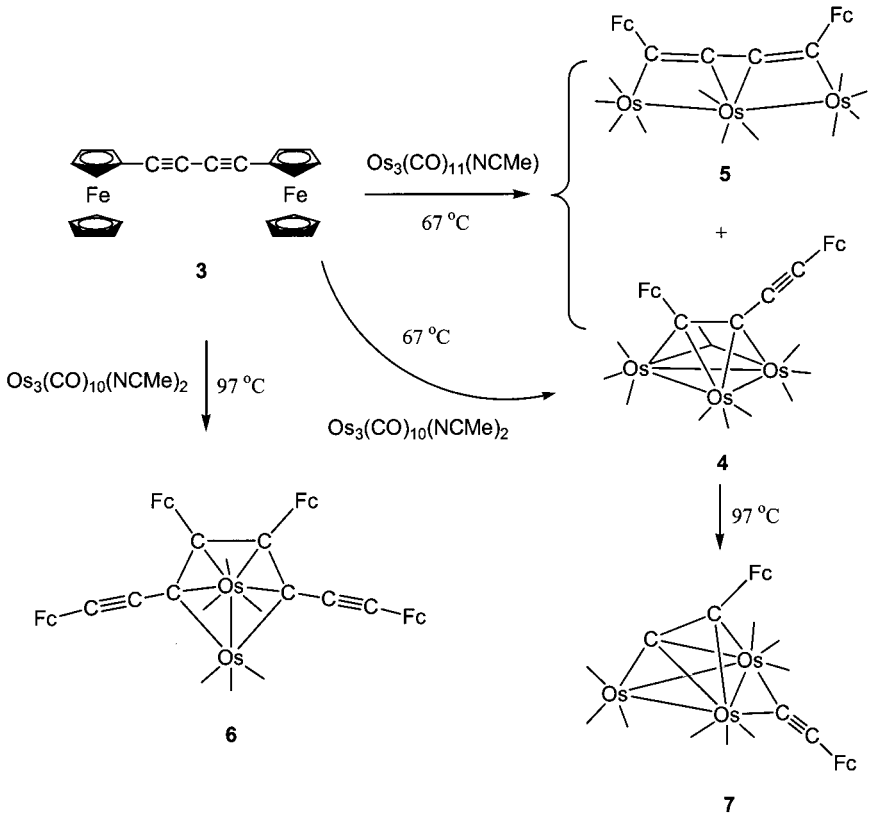

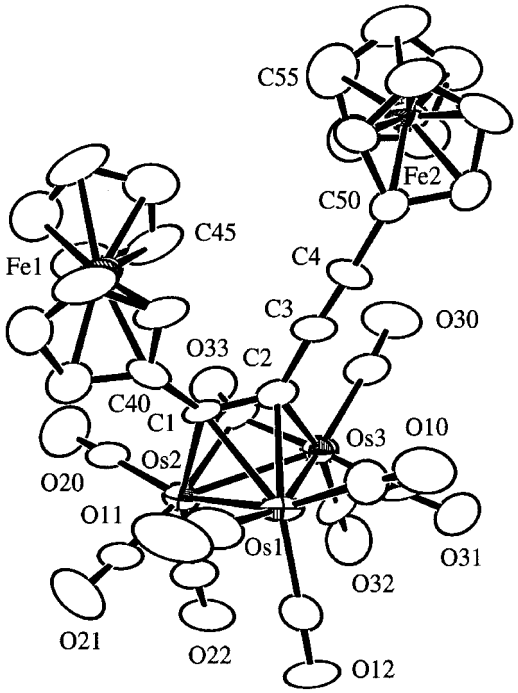

Figure 1. ORTEP diagram of $Os_3(CO)_{10}(\mu_3\text{-}\eta^2\text{-}FcC_4Fc)$ (**4**) showing 40% probability thermal ellipsoids.

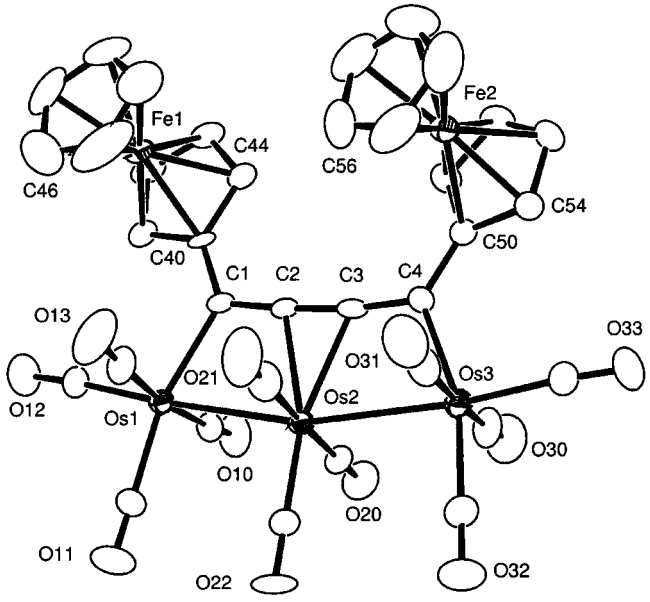

Figure 2. ORTEP diagram of $Os_3(CO)_{11}(\mu_3\text{-}\eta^4\text{-}FcC_4Fc)$ (**5**) showing 40% probability thermal ellipsoids.

in the ^1H NMR spectrum for the C_5H_5 rings of the two Fc ligands: δ 4.17 ppm.

When the reaction of **2** with **3** was performed at 97 °C for 6 h, the new compound **6** was obtained as a minor product in 9% percent yield. Compound **6** was characterized crystallographically. Selected interatomic distances and angles for **6** are listed in Table 2. An ORTEP diagram of the molecular structure of **6** is shown in Figure 3. Compound **6** is a member of the well-known ferrole-type binuclear metallacyclopentadiene series. Two molecules of 1,4-bis(ferrocenyl)butadiyne ligands are coupled "head-to-head" by using one of their two triple bonds to form the metallacycle. The structure study shows that the osmacyclopentadiene ring is substituted by the ferrocenyl groups in the 3,4-positions and by the FcC≡C groups in the 2,5-positions.

When compound **4** was heated to 97 °C for 3.5 h, the new compound **7** was obtained as the only product in 91% yield. Selected interatomic distances and angles for

Table 2. Selected Bond Lengths (Å) and Angles (deg) from Compounds 4−7[a]

	4	5	6	7
		Distances		
Os1−Os2	2.7456(9)	2.9032(4)	2.7556(7)	3.184(1)
Os2−Os3	2.8328(8)	2.9031(5)		2.864(1)
Os1−Os3	2.7956(8)			2.857(1)
Os1−C1	2.33(1)	2.150(8)	2.276(10)	2.26(2)
Os1−C2	2.21(1)		2.352(10)	2.24(2)
Os1−C3				2.19(2)
Os1···C4				3.266
Os1−C5			2.349(9)	
Os1−C6			2.272(9)	
Os2−C1	2.13(1)			2.28(2)
Os2−C2		2.335(7)	2.084(10)	2.28(2)
Os2−C3		2.323(8)		2.27(2)
Os2···C4				3.045
Os2−C6			2.099(10)	
Os3−C2	2.12(2)			1.95(2)
Os3−C4		2.152(8)		
C1−C2	1.40(2)	1.328(11)	1.426(14)	1.38(3)
C2−C3	1.47(2)	1.324(11)	1.446(15)	
C3−C4	1.19(2)	1.319(12)	1.176(14)	1.19(3)
C1−C5			1.484(13)	
C5−C6			1.412(14)	
C6−C7			1.439(14)	
C7−C8			1.182(14)	
		Angles		
Os1−Os2−Os3	60.12(2)	162.632(15)		56.08(3)
Os2−Os1−Os3	61.47(2)			56.28(3)
Os1−Os3−Os2	58.41(2)			67.64(3)
C2−C1−C40	126(1)	121.8(7)		136(2)
C1−C2−C3	124(1)	173.5(9)	120.8(9)	
C2−C3−C4	173(1)	172.6(8)	168.9(12)	
C3−C4−C50	177(2)	122.9(7)		173(2)
C5−C6−C7			121.1(9)	
C6−C7−C8			172.1(11)	
Os1−C3−Os2				90.9(7)
Os3−C2−C1				148(2)

[a] The estimated standard deviation in the least significant figure is given in parentheses.

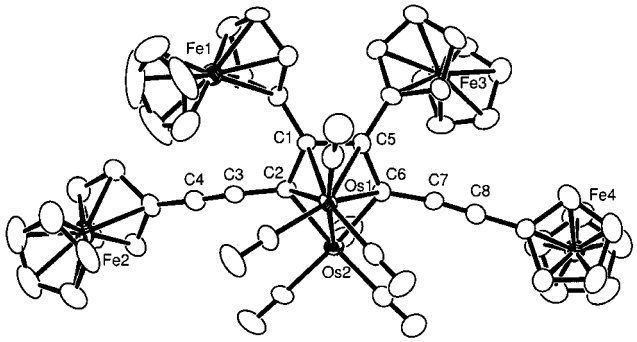

Figure 3. ORTEP diagram of $Os_2(CO)_6(\mu_4\text{-}\eta^4\text{-}FcC_2C{\equiv}CFc)_2$ (**6**) showing 40% probability thermal ellipsoids.

7 are listed in Table 2, and an ORTEP diagram of the molecular structure of **7** is shown in Figure 4. The structure of **7** is similar to the family of bis(alkynyl) complexes $Os_3(\mu_3\text{-}C_2R^1)(\mu_2\text{-}C_2R^2)(CO)_9$ ($R^1 = R^2 =$ Ph; $R^1 = R^2 =$ $SiMe_3$; $R^1 =$ $SiMe_3$, $R^2 =$ Ph), which have been obtained by cleavage of the central carbon−carbon bond of the other osmium diyne cluster complexes $Os_3(R^1C_2C_2R^2)(CO)_{10}$.[15] In **7** one of the acetylide ligands is coordinated to the metals in an $\mu_3\text{-}\eta^2$ coordination mode. The other acetylide is coordinated to Os(1) and Os(2) in

(15) (a) Deeming, A. J.; Felix, M. S. B.; Bates, P. A.; Hursthouse, M. B. *J. Chem. Soc., Chem. Commun.* **1987**, 461. (b) Deeming, A. J.; Felix, M. S. B.; Nuel, D. *Inorg. Chim. Acta* **1993**, *213*, 3.

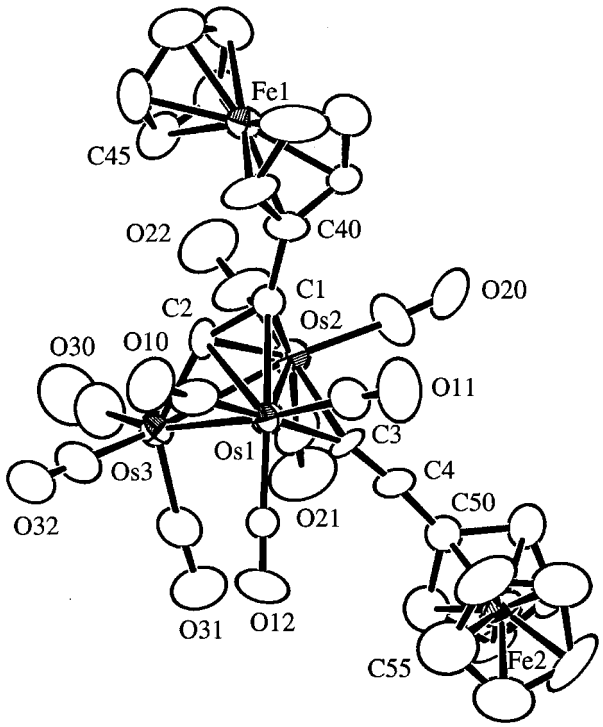

Figure 4. ORTEP diagram of $Os_3(CO)_9(\mu_3\text{-}\eta^2\text{-}C{\equiv}CFc)(\mu\text{-}\eta^2\text{-}C{\equiv}CFc)$ (**7**) showing 40% probability thermal ellipsoids.

a $\mu\text{-}\eta^1$ mode. The μ_3-bridged alkyne is considered to be a σ + di-π bonding mode. These ligands are generally regarded as 5e donors. The edge-bridged alkyne is bonded to Os(1) and Os(2) in a σ coordination fashion, and the two π bonds are not coordinated. If this ligand is regarded as a neutral 1e donor, then the cluster has a total of 48e, which is the number expected for an electron-precise triangular cluster containing three metal−metal bonds. The Os(1)−Os(3) and Os(2)−Os(3) bonds distances are normal: 2.857(1) and 2.864(1) Å, respectively. The Os(1)−Os(2) distance is slightly long, 3.184(1) Å, but this could still be considered to be a bonding interaction.

The decarbonylation of triosmium clusters containing diyne ligands, $Os_3(R^1C_2C_2R^2)(CO)_{10}$, does not always result in cleavage of the C−C bond between the two alkyne groups. For example, when heated, $Os_3(CO)_{10}(EtC_2C_2Et)$ is converted to the allenyl cluster complex $[Os_3H(\mu_3\text{-}\eta^2\text{-}\eta^2\text{-}MeCH{=}C{=}CC_2Et)(CO)_9]$ by cleavage of C−H.[15b] It has been suggested that the cleavage of the central carbon−carbon bond depends on the nature of the substitutents at the 1- and 4-positions. The cleavage of the diyne ligand occurs in the absence of α-hydrogen atoms, but C−H cleavage is favored if they are present.[15b]

The electrochemical data for compounds **3**−**7** are listed in Table 3. The differential pulse (DP) voltammogram of compound **4** shows two poorly resolved one-electron oxidations for the ferrocenyl groups at E_p = 0.483 and 0.540 V vs Ag/AgCl (ΔE_p = 0.057 V).[7] Interestingly, compound **5** shows two well-resolved one-electron oxidations for the ferrocenyl groups at E_p = 0.300 and 0.484 V vs Ag/AgCl (ΔE_p = 0.184 V).[7] The redox potentials of diyne **3** shows two one-electron oxidations with the separations E_p = 0.48 and 0.58 V vs Ag/AgCl (ΔE_p = 0.10 V), which is intermediate to those of the two cluster complexes. Compound **6** shows two oxidation peaks for the four ferrocenyl groups, a

Downloaded by CARLI CONSORTIUM on June 29, 2009
Published on May 25, 2002 on http://pubs.acs.org | doi: 10.1021/om0201213

Table 3. Electrochemical Data for Compounds 3−7[a]

	peak positions				
compd	$E_p(+/0)$[b]	$E_p(2+/+)$[b]	$E_{1/2}(+/0)$[c]	$E_{1/2}(2+/+)$[c]	ΔE_p[d]
3	0.476	0.576	0.486	0.586	0.100
4	0.483	0.540	0.493	0.550	0.057
5	0.300	0.484	0.310	0.494	0.184
6	0.364	0.512	0.389	0.537	0.148
7	0.430	0.650	0.455	0.675	0.216

[a] The data were recorded on a CV-50W voltammetric analyzer with 1.0 mM sample in a 0.1 M $^nBu_4NPF_6$ solution (CH_2Cl_2/NCMe 1:1) with carbon working and Pt counter electrodes and a Ag/AgCl reference electrode. The scan rate is 100 mV/s for CV and 20 mV/s for DPV. Under these conditions E_p for ferrocene was recorded at 0.320 V (using $E_{pul} = 10$ mV). All values are given in V. [b] E_p is peak position in DPV. [c] $E_{1/2} = E_p + E_{pul}/2$.[13] $E_{pul} = 10$ mV from DPV for **3**−**5**; $E_{pul} = 50$ mV for **6** and **7**. [d] $\Delta E_p = E_p(2+/+) - E_p(+/0)$.

broad oxidation peak at $E = 0.512$ V and a shoulder at $E = 0.364$ V ($\Delta E_p = 0.148$ V). Compound **7** shows two well-resolved one-electron oxidations for the ferrocenyl groups at $E_p = 0.43$ and 0.65 V vs Ag/AgCl ($\Delta E_p = 0.22$ V).

Discussion

The coordination of alkyne groups to triangular clusters, such as that in **4**, has been well studied and will not be discussed further here.[16] The coordination of adjacent alkyne groups in a parallel mode as found in **5** is heretofore unprecedented. It is similar to that observed for cis-dimetalated olefins,[17] and it is tempting to describe **5** as bis-cis-dimetalated olefin or substituted butadiene (**A**), where Os(1) and Os(3) are σ-bonded to

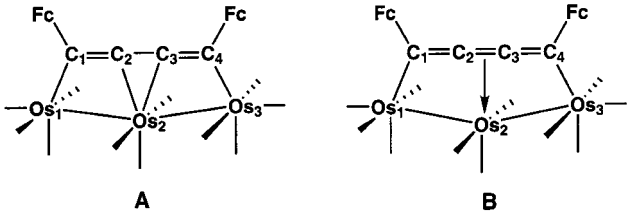

C(1) and C(4) and the central osmium atom, Os(2), is connected to C(2) and C(3), also in a σ fashion. In this case, one might expect that the C(2)−C(3) bond distance should be longer than the C(1)−C(2) and C(3)−C(4) distances. In fact, they are all the same within experimental error: 1.319(12)−1.328(11) Å. There is an alternative way to represent the electronic structure of this compound, and it is shown in **B**. Again C(1) and C(4) are σ-bonded to the two end osmium atoms; however, the C(2)−C(3) unit is π-bonded to Os(2). The organic ligand can be considered to be a bis(dehydrobutatriene) (**C**). There are two lone pairs and one π orbital in the plane of the Os_3 chain. Two π bonds are left perpendicular to the Os_3C_4 plane. Using the isolobal analogy,[18,19] the two end Os groups are then counted as $Os(CO)_4^+$ d^7 ML_4 fragments. There are two frontier orbitals with one electron on each fragment to be used for the Os−Os bonding. The central $Os(CO)_3$ group can be thought of as a d^8 ML_3 fragment. There is one empty frontier orbital pointed toward the central C−C π bond in the butatriene ligand, which is the basic bonding description given for a d^8 square-planar olefin−ML_3 complex. There are also two more important orbitals at the "square planar" coordination site. These, as shown in **C**, will be used to form two Os−Os σ bonds. From the perspective of a square-planar complex the two orbitals are z and z^2, as shown in **D**.

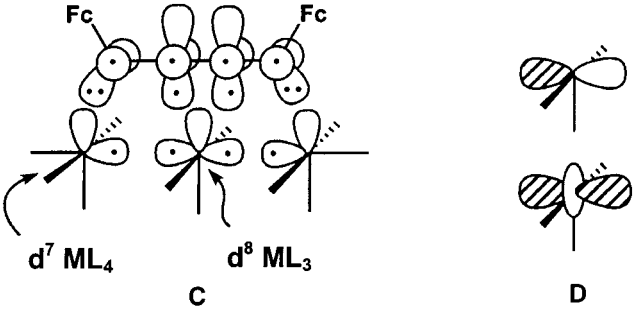

The question of whether it is better to represent a complex as a metallacyclopropane (**A**) or a metal−olefin (**B**) is an old one.[20] Basically, it is a matter of whether back-bonding from a filled metal d orbital to olefin π^* is substantial (as it is in a metallacyclopropane) or not. In the present case, there are two unusual structural features, as we shall see, that have a direct bearing on this issue and on the electronic structure for the molecule: the Os(2)−C(2) and Os(2)−C(3) distances of 2.335(7) and 2.323(8) Å, respectively, are considerably longer than the two Os(1)−C(1) and Os(3)−C(4) distances of 2.150(8) and 2.152(8) Å, respectively, which are certainly best described as σ bonds. Second, the Os−Os−Os chain bends by an angle of 162.632(15)° away from the butatriene ligand. To investigate the details of the electronic structure, we have carried out extended Hückel calculations on this molecule, where the ferrocenyl groups have been replaced by hydrogen atoms.

Let us start the discussion by construction of the important valence orbitals associated with the bis(dehydrobutatriene) ligand. The dominant interaction in the Os_3 cluster will be from the two lone pairs and the two π MOs, which lie in the Os_3 chain. The four perpendicular π orbitals (with four electrons) interact with the Os_3 chain to a lesser degree and will be discussed later. The symmetric and antisymmetric combination of lone pair orbitals (n_s and n_a) will interact with the π and π^* orbitals, respectively, to form four MOs. These are shown in Figure 5 along with contour drawings of the resultant MOs. The π orbital, $1a_1$, is stabilized by interaction with n_s, making it a poorer σ-donor. On the other hand, the antibonding combination, $2a_1$, which is predominately n_s, becomes a better σ donor. What is more important to the ensuing discussion is that the n_a lone pair combination interacts with and destabilizes π; therefore, the π-acceptor ability of the $2b_2$ MO is diminished. The important valence orbitals of the $Os_3(CO)_{11}^{2+}$ fragment are also easy to

(16) Shilling, B. E. R.; Hoffmann, R. *J. Am. Chem. Soc.* **1979**, *101*, 3456.
(17) (a) Burke, M. R.; Takats, J. *J. Organomet. Chem.* **1986**, *302*, C25. (b) Dickson, R. S.; Johnson, S. H.; Kirsch, H. P.; Lloyd, D. J. *Acta Crystallogr.* **1977**, *B33*, 2057. (c) Clemens, J.; Green, M.; Kuo, M.-C.; Fritchie, C. J.; Mague, J. T.; Stone, F. G. A. *J. Chem. Soc., Chem. Commun.* **1972**, 53. (d) Davidson, J. L.; Harrison, W.; Sharp, D. W. A.; Sim, G. A. *J. Organomet. Chem.* **1972**, *46*, C47. (e) Koie, Y.; Shinoda, S.; Saito, J.; Fitzgerald, B. J.; Pierpont, C. *Inorg. Chem.* **1990**, *9*, 2350.
(18) Hoffmann, R., *Angew. Chem.* **1982**, *94*, 725; *Angew. Chem., Int. Ed. Engl.* **1982**, *21*, 711.
(19) Albright, T. A.; Burdett, J. K.; Whangbo, M.-H. *Orbital Interactions in Chemistry*; Wiley: New York, 1985.
(20) Reference 19, pp 367−368.

Downloaded by CARLI CONSORTIUM on June 29, 2009
Published on May 25, 2002 on http://pubs.acs.org | doi: 10.1021/om0201213

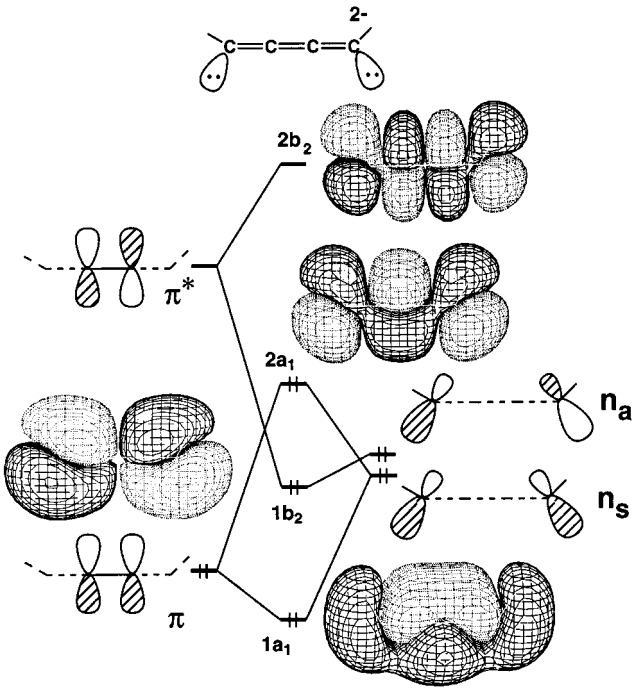

Figure 5. Interaction diagram for building up the in-plane MOs in the bis(dehydrobutatriene) dianion. The symmetry-adapted combinations of the two lone pairs at the ends are given on the right side, and the central π and π^* orbitals are shown on the left side. Contour plots of each resultant MO are given, where the solid and dashed lines refer to positive and negative amplitudes in the wavefunction.

determine. Each end $Os(CO)_4^+$ fragment possesses two valence orbitals, **E** and **F**.[17,18] The symmetric and

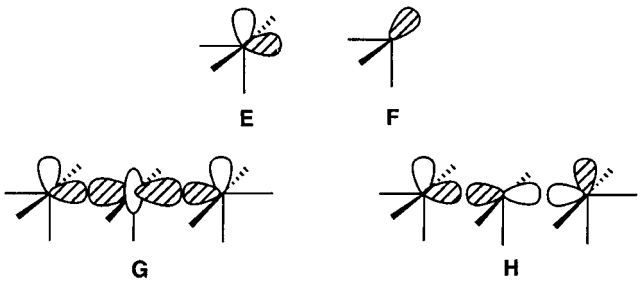

antisymmetric combinations of **E** along with **D** are primarily responsible for forming the two filled Os−Os bonding MOs, **G** and **H**. Left over then is the s and p hybrid orbital (**F**) at each end along with the hybrid orbital at the central Os, which points toward the π orbital in the butatriene ligand (see **C**). The three empty fragment orbitals form combinations, two of which have a_1 symmetry and one which has b_2 symmetry. These three lowest unoccupied MOs of $Os_3(CO)_{11}^{2+}$ are shown in Figure 6 along with their stylized representations in the lower left corner. A completely equivalent way to view the $Os_3(CO)_{11}^{2+}$ fragment is to consider each metal as being part of a d^6 ML_5 unit. There is one frontier orbital which points toward the missing site of each octahedron, and this orbital is empty.[18,19] Again symmetry-adapted combinations lead to the pattern presented in Figure 6. In any case it is important to note that the lowest orbital, $1a_1$, contains no nodes along the Os−Os−Os chain, the $1b_2$ orbital contains one node perpendicular to the chan, and finally, the $2a_1$ orbital has two perpendicular nodes.

The construction of the important MOs in the $(C_4H_2)Os_3(CO)_{11}$ molecule is now an easy matter. This is done in Figure 7. The three filled orbitals in the butatriene ligand find perfect matches, in terms of symmetry and topology, with the three empty $Os_3(CO)_{11}^{2+}$ fragment orbitals to produce the three bonding molecular orbitals. We note in particular that the $1a_1$, $1b_2$, and $2a_1$ orbitals of the butatriene ligand have zero, one, and two perpendicular nodes, respectively, and these neatly match those from the Os_3 chain. From a localized perspective the three resultant MOs are the two Os−C σ bonds and the dative π bond from the central olefin to the central osmium atom. Back-donation from metal to the central olefin takes place via the metal d orbital shown in **I**. However, as indicated in Figure 6, the $2b_2$

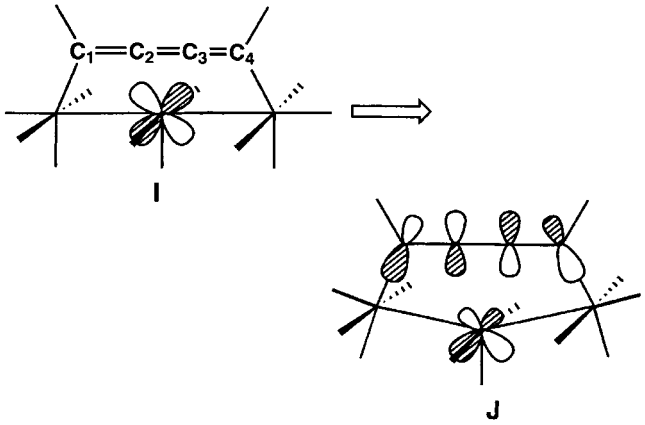

MO lies high in energy and consequently will not interact strongly with **I**. Furthermore, the filled MO, $1b_2$, overlaps strongly with **I**, and therefore, this represents a two-orbital−four-electron destabilizing interaction. A way to alleviate this repulsion is to bend the Os(1)−Os(2)−Os(3) chain so that Os(2) moves away from the butatriene ligand. There are two ramifications associated with this motion. First, the Os(2) d AO in **I** becomes hybridized away from the butatriene ligand and consequently overlaps less with the $1b_2$ π orbital (and $2b_2$). Second, the Os(2)−C(2) and −C(3) distances become longer, which, of course, also decreases the overlap with $1b_2$ and $2b_2$. Thus, the bending motion supports the notion that there is little back-bonding in the complex. One could contend that the bending motion serves to reorient the hybrid orbitals at Os(1) and Os(3) so that the σ bonding to C(1) and C(4) becomes stronger. This is as observed in **5** and is also seen in our calculations. However, as we indicated before, the Os(2)−C(2) and −C(3) distances, at an average of 2.329(8) Å, are appreciably longer than normal. The mean Os−C bond length for olefin−Os complexes (four examples) reported prior to 1989 was 2.18 Å with a standard deviation of 0.03 Å.[21] There are a number of more recent structures, and they also have similar distances: for example, in ethylene−$Os(CO)_4$ the two Os−C distances are 2.221(10) Å[22] and in $(ethylene)_2(H)Os(PMe_2Ph)_3^+$ the distances range from 2.22 to 2.242(6) Å.[23] Thus, the distances in our compound

(21) Orpen, A. G.; Brammer, L.; Allen, F. H.; Kennard, O.; Watson, D. G. *J. Chem. Soc., Dalton Trans.* **1989**, S1.
(22) Bender, B. R.; Norton, J. R.; Miller, M. M.; Anderson, O. P.; Rappe, A. K. *Organometallics* **1992**, *11*, 3427.

Downloaded by CARLI CONSORTIUM on June 29, 2009
Published on May 25, 2002 on http://pubs.acs.org | doi: 10.1021/om0201213

Downloaded by CARLI CONSORTIUM on June 29, 2009
Published on May 25, 2002 on http://pubs.acs.org | doi: 10.1021/om0201213

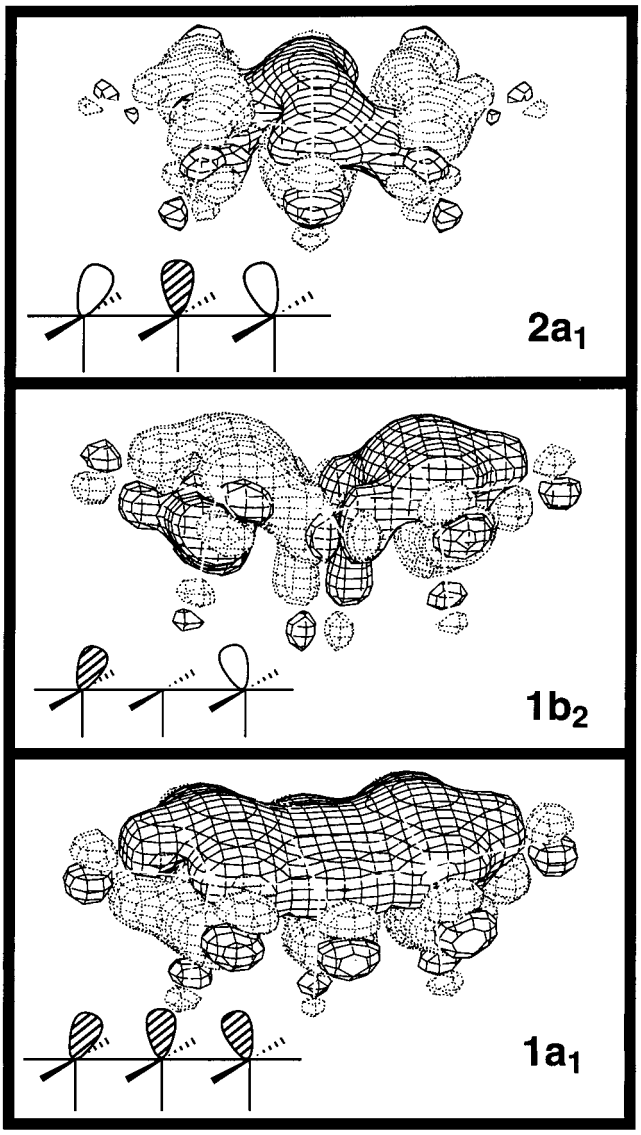

Figure 6. Contour diagrams for the three lowest unoccupied MOs in $Os_3(CO)_{11}^{2+}$.

appear to be very long, which is consistent with our analysis that there is π bonding from C(2) and C(3) to Os(2) but there is little back-bonding, and the representation indicated by **B** is more appropriate than that in **A**.

The electrochemical measurements show that the two redox processes for the ferrocenyl groups in **5** are separated much farther ($\Delta E_p = 0.184$ V) than those in the free molecule **3** ($\Delta E_p = 0.100$ V) and the separation of the two redox processes in **4** is the smallest of these three compounds ($\Delta E_p = 0.057$ V). There are two possible explanations for these changes. One of these could be simple electrostatic "Coulombic" effects on noninteracting (noncommunicating) redox centers, but we believe that electrostatic effects can be ruled out for two reasons: (1) electrostatic effects between noninteracting ferrocenes should be only about 0.036 V,[24] and (2) electrostatic effects vary as $1/d^2$, where d is the distance between the centers, and would produce increased separation of the redox events as the distance between the two redox centers is decreased.[25] While it is true that the distance between the two iron atoms in **5** (6.09 Å) is significantly less than that in **3** (9.90 Å), the distance between the iron centers in **4** (6.25 Å) is virtually the same as that in **5**. If electrostatic effects are responsible for the changes in the redox processes of **4** and **5**, then the separation between the redox processes for both should be similar and *both should be larger than that of 3*. This is contrary to the observations. Alternatively, the most likely explanation for the differences between the redox potentials of **3**−**5** is some form of "electrocommunication" and we propose that it occurs through modifications in the π-orbital network of the diyne ligand that are induced by the metal atoms. Recall from the bonding description in **C** that there are four perpendicular p AOs and four electrons to put into the π MOs of the ligand. These MOs are topologically analogous to those in butadiene, with the important difference that the C(2)−C(3) distance is very short in this bis(dehydrobutatriene) ligand, whereas the analogous difference in butadiene, as well as that for the starting ligand **3**, is quite long—typical of that for a C−C single bond. It is this enhanced π-bonding between C(2) and C(3) that leads to greater communication between the ferrocenyl groups. With reference back to the interaction diagram in Figure 7, there are two filled π orbitals, $1b_1$ and $2b_1$. They interact with nonbonding d MOs on the Os trimer in primarily a bonding and antibonding manner, respectively. Contour plots of the

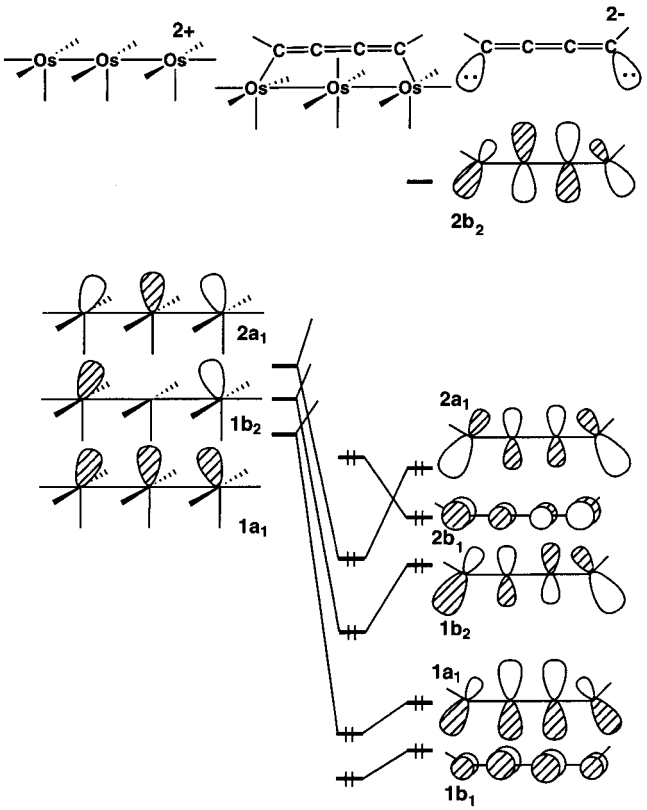

Figure 7. Orbital interaction diagram for the $(C_4H_2)Os_3(CO)_{11}$ complex in terms of the important valence orbitals of the bis(dehydrobutatriene(2−)) ligand (right) and $Os_3(CO)_{11}^{2+}$ fragment (left).

(23) Johnson, J. J.; Huffman, J. C.; Caulton, K. G.; Jackson, S. A.; Eisenstein, O. *Organometallics* **1989**, *8*, 2073.
(24) Flanagan, J. B.; Margel, S.; Bard, A. J. *J. Am. Chem. Soc.* **1978**, *100*, 4248.
(25) Cotton, F. A.; Donahue, J. P.; Lin, C.; Murillo, C. A. *Inorg. Chem.* **2001**, *40*, 1234.

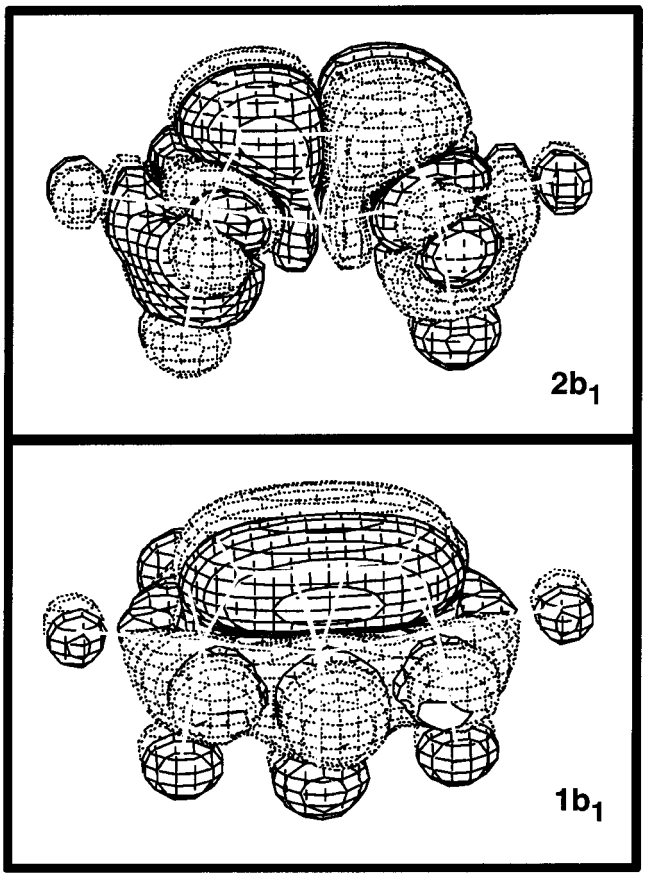

Figure 8. Contour diagrams for the $1b_1$ and $2b_1$ MOs (see Figure 7) in $(C_4H_2)Os_3(CO)_{11}$.

two resultant MOs are provided in Figure 8, and they clearly demonstrate mixing between the butatriene MOs and the orbitals on Os. What is germane to this discussion is that the $2b_1$ MO in particular lies high in energy and will also overlap and interact strongly with a combination of the ferrocenyl nonbonding orbitals.[19] Consequently, one ionization potential will be well separated from the other. It is this mechanism, the coupling via the $2b_1$ MO, that provides a delocalized view for the enhanced communication between the two ferrocenyl groups.

For compound **4**, the separation between the two ferrocenyl redox processes is smaller than that of the free molecule **3** ($\Delta E_p = 100$ mV). This is despite the fact that two ferrocenyl groups in **4** are also inequivalent, which should increase the difference in their redox potentials. In **4** it is found that both π bonds of a single alkyne group are coordinated to the triangular cluster. The two π orbitals of the alkyne are, therefore, used primarily for the formation of Os−C bonds. Furthermore, the C(2)−C(3) bond between the coordinated and uncoordinated alkyne group is longer than that in both **3** and **5**. Thus, if electrocommunication is based on π interactions, then one might expect the communication to be smaller in **4**. This is consistent with the electrochemical observations. We have recently reported that the reaction of **1** with 1,8-bis(ferrocenyl)octatetrayne leads to the formation of a similar open cluster, $Os_3(CO)_{11}(\mu_3\text{-}\eta^4\text{-}FcC_4C{\equiv}CC{\equiv}CFc)$, as observed in the compound **5**.[26]

Complexes of the structural type of **6** are quite frequently formed by the coupling of alkynes in reactions with iron and ruthenium carbonyls,[27] but few have been characterized in the osmium family of compounds. Compound **6** is obviously formed by a symmetric coupling process. We found no evidence for formation of the unsymmetrically coupled product. The DP voltammogram shows a broad oxidation peak at 0.512 V and a shoulder at 0.364 V. The large difference in the redox potentials can be attributed to the intrinsic inequivalence in the two types of ferrocenyl groups.

The formation of **7** from **4** involves a cleavage of the central C−C bond. It was not established whether the alkyne coordinated in the μ_3 position in **4** became the μ_3-alkynyl group in the cleaved product or if the uncoordinated diyne somehow migrated to the μ_3 position in the cleaved product. At present, we have no evidence for interconversions between the μ_3-alkynyl and μ_2-alkynyl groups.[15b] The difference between the oxidation potentials of the ferrocenyl groups in compound **7** is the largest all of these compounds; $\Delta E_p = 0.22$ V. This does not imply, however, that there is an increase in electronic communication between the ferrocenyl groups, because the two ferrocenyl groups are inequivalent. The intrinsic inequivalence of two ferrocenyl groups can contribute to the value of ΔE by an amount that cannot be determined.

Summary

We have established a new linear coordination mode for conjugated diynes to trimetallic groups. The coordination of the metals induces a triene character into the diyne that facilitates electrocommunication through the unsaturated carbon chain, as indicated by the redox response of appended ferrocenyl groups.

Acknowledgment. This work was supported by a Research Investment award from the University of South Carolina. T.A.A. thanks the Robert A. Welch Foundation for support of this work.

Supporting Information Available: Figures giving cyclic voltammograms and tables giving X-ray crystallographic data for the structural analyses of **4**−**7**. This material is available free of charge via the Internet at http://pubs.acs.org.

OM0201213

(26) Adams, R. D.; Kwon, O.-S.; Qu, B.; Smith, M. D. *Organometallics* **2001**, *20*, 5225.

(27) (a) Fehlhammer, W. P.; Stolzenberg, H. In *Comprehensive Organometallic Chemistry*; Wilkinson, G., Stone, F. G. A., Abel, E., Eds.; Pergamon Press: Oxford, U.K., 1982; Chapter 31.4.2.2.4. (b) Koridze, A. A.; Yanovsky, A. I.; Struchkov, Yu. T. *J. Organomet. Chem.* **1992**, *441*, 277. (c) Bruce, M. I.; Zaitseva, N. N.; Skelton, B. W.; White, A. H. *Inorg. Chim. Acta* **1996**, *250*, 129. (d) Adams, R. D.; Qu, B.; Smith, M. D. *Inorg. Chem.* **2001**, *40*, 2932.

Downloaded by CARLI CONSORTIUM on June 29, 2009
Published on May 25, 2002 on http://pubs.acs.org | doi: 10.1021/om0201213